ChemPlusChem

A Multidisciplinary Journal Centering on Chemistry

Chemistry Europe

European Chemical Societies Publishing

Accepted Article

Title: A Sustainable Palladium Intercalated Montmorillonite Clay Catalytic System for Imine Hydrogenation under Mild Conditions

Authors: Unnati Gupta, Krishnapriya R, and Rakesh K Sharma

To be cited as: *ChemPlusChem* 10.1002/cplu.202000760

Link to VoR: https://doi.org/10.1002/cplu.202000760

WILEY-VCH

WILEY-VCH

FULL PAPER

A Sustainable Palladium Intercalated Montmorillonite Clay Catalytic System for Imine Hydrogenation under Mild Conditions

Unnati Gupta,[a] Dr. R. Krishnapriya [a] and Prof. Rakesh K Sharma *[a]

[a] Unnati Gupta, Dr. R. Krishnapriya and Prof. Rakesh K Sharma*
Sustainable Materials and Catalysis Research Laboratory (SMCRL), Department of Chemistry
Indian Institute of Technology Jodhpur
Jodhpur, Rajasthan India-342037
rks@iitj.ac.in.
Supporting information for this article is given via a link at the end of the document

Abstract: Herein, we report a series of palladium nanoparticles (Pd NPs) intercalated montmorillonite clay catalysts for hydrogenation of 3-diphenyl prop-2-en-1-imine under mild reaction conditions. Pd/Clay catalyst was prepared by a simple wet-impregnation method, and the physicochemical properties were characterized extensively by various techniques including N_2 adsorption, XRD, TEM, XPS and TPR etc., which showed the intercalation of active Pd NPs between the clay layers. Effect of reaction conditions such as catalyst loading, reaction time, temperature and H_2 pressure is explored, thereby a plausible mechanism is proposed. The optimum amount of 6 wt% Pd/Clay catalyst displayed significant catalytic activity to yield 3-phenyl propyl aniline with 100 % conversion and selectivity under 5 bar pressure for shorter reaction period of 3.5 h at 100 °C. The developed catalytic system unveiled excellent reusability over five cycles and hence paved the way for industrial applications.

Introduction

Considering ever-growing environmental cognizance, a sustainable green chemistry route to synthesize fine chemicals is challenging and appeals to significant attention worldwide.[1] Homogeneous catalysts offer unique advantages in terms of high activity and selectivity; however, the catalyst recovery process for an industrial scale requires laborious purification, which is economically unviable.[2] Moreover, the catalyst recovery process often generates a large amount of leftover chemicals which is detrimental from the perspective of green chemistry.[3] Therefore, heterogeneous catalysts are preferred as they allow the isolation of catalytic sites resulting in facile separation and catalyst reuse.[4] The catalytic hydrogenation of imines is a clean and environmentally benign methodology. The resultant amines are necessary fine-chemicals that serve as building blocks for various agrochemical and pharmaceutical products. [5] Several metal-based heterogeneous catalysts including platinum group metals (PGM), first-row transition metals, alkali and alkaline earth metals have been reported for hydrogenation reactions.[6]. Considering the cost-effectiveness first-row transition metals are preferred, but they require high H_2 pressure and reaction temperature to break the metal-hydrogen (M-H) bond. In addition, the 3d metals tendency to engage in radical chemistry make them a less attractive candidate. In the case of alkali metals, the absence of vacant d orbital leads to severe substrate activation and low product selectivity.[5a] In this regard, the noble metal palladium offers a viable solution as it has weak Pd-H bond strength, availability of vacant d orbitals and can dissolve a large amount of hydrogen in its crystal lattice.[7] However, due to its high cost and affinity to agglomeration, there is a growing demand to use palladium catalyst with minimum loading, high turnover number (TON) and excellent recyclability. To achieve this, the idea to immobilize Pd nanoparticles (NPs) on suitable support is receiving significant consideration.[8]

The performance of supported metal catalyst depends mainly on the nature of support material, metal-support interaction and also the metal particle size.[9] Moreover, the support should be capable of reducing the metal agglomeration by controlling its size without passivation of the active surface.[10] Therefore, various supports such as zeolites[11], carbon nanotube[12], activated carbon[13], silica[14] etc. have been reported. Most of these supports have low thermal stability, require excess organic solvents and complex preparation procedure and that adds extra cost to the immobilization process. [11] Accordingly, the development of a heterogeneous optimized catalyst system that could accomplish organic transformations at ambient reaction conditions using benign solvent systems is highly preferred.

Recently, clay has emerged as a ubiquitous support material owing to its lamellar structure and mechanical/thermal stability.[15] The low-cost, ordered layered structure, unique swelling, intercalation and high ion exchange property make this clay a suitable candidate to use as a promoter, catalyst precursor and also as a good support.[16] The outstanding feature of clay is that H_2O and other organic/inorganic entities can enter between unit layers resulting in expansion of lattice in *c*-direction.[17] These layers are functionalized by cation exchange by isomorphous substitution, which causes charge imbalance. This is balanced by interlayer compensatory hydratory cations such as Na^+, Ca^{2+} and Mg^{2+}, which on further exchange introduces the catalytically active materials to layers.[18] Moreover, acid treatment with dilute acids like HNO_3 resulted in the relocation of Al in interlayer spacing which acts as brønsted sites, thus modifying acidic centres.[19]

In recent years' various clay minerals have been used as a robust support for palladium to carryout important organic transformations considering its low cost, simple preparation method and remarkable reusability.[20] For instance, palladium based bifunctional metal-acid catalyst supported on K-10 acidic clay was used to transform HMF into 2,5-dimethyl furan (2,5-DMF)[21], while Sreekumar et al. used clay-supported Pd catalyst for the regioselective arylation of 3,4-ethylenedioxythiophene.[22] Montmorillonite clay play a key role in the Pd catalysed furfural hydrogenation to give 1,2-pentanediol (1,2-PeDO) with 66% selectivity[23]. Another significant work reported is the Pd-supported halloysite nanoclay (PdM@Hal) for efficient methane oxidation.[24] Apart from these reports, the applicability of clay for palladium-based catalyst can be understood from the enormous

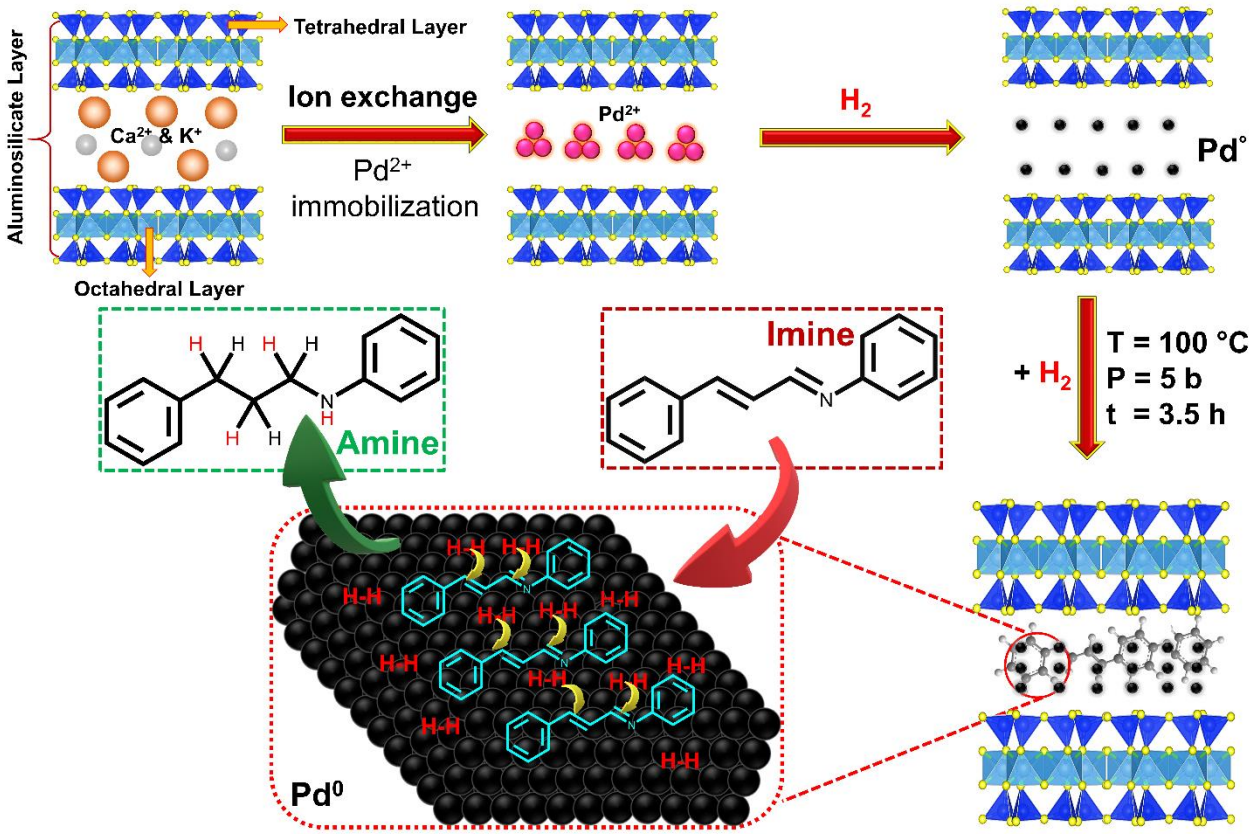

Scheme 1. Schematic representation of Pd NPs intercalated clay synthesis and proposed working mechanism of the interaction of Pd NPs with adsorbed H_2 and substrate imine.

application in numerous coupling reaction such as Suzuki-Miyaura,[25] Ullmann coupling,[26] Sonogashira Reaction,[27] Heck–Mizoroki reactions[28] etc. Moreover, we have also studied the effective utilization of Pd NPs[29] and Ni/Co intercalated montmorillonite clay[30] as green catalysts for the chemo selective hydrogenation of squalene into squalane and for the conversion of microalgae oil to diesel-grade hydrocarbons. In this continuation of our research of developing green synthesis protocols, we herein propose the use of montmorillonite clay as a robust support for immobilization of Pd NPs and its application potential for catalytic hydrogenation of imines. The influence of reaction conditions (catalyst loading, H_2 pressure, reaction time, temperature) and recycling on the structural modification, activity and selectivity of the desired product is investigated in detail. The study also includes extensive characterization of prepared catalyst that quantifies its synthetic efficiency and is expected to have a profound impact in the field of sustainable catalysis.

Results and Discussion

The characterization studies of Pd intercalated clay catalyst and their significance in hydrogenation studies were started primarily with its preparation using natural clay. The general formula of clay used in this study is $K_3Ca_1Ti_{0.6}Al_{12}Si_{40}Fe_6H_xO_y$ and was calculated by collective X-ray fluorescence (XRF) spectrometry and scanning electron microscopy coupled with energy dispersive X-ray (SEM/EDX) spectroscopy reported in our previous report.[29] The natural clay is composed of montmorillonite where octahedral AlO_6 sheets are sandwiched between two tetrahedral SiO_4 sheet as shown in **Scheme 1**. The interlayer space is occupied by K^+ and Ca^{2+} ions coordinated by H_2O molecule. The Pd intercalation in natural clay was achieved by a simple wet impregnation method in dilute nitric acid. Generally, during intercalation, swelling of clay occurs which facilitates the cation exchange leading to the effective incorporation of Pd^{2+} ions between the clay interlayers. The incorporated Pd^{2+} ions on calcination under hydrogen atmosphere lead to catalytically active Pd^0 NPs.[31] The detailed mechanism of intercalation is illustrated in **Scheme 1**. Accordingly, natural clay-based catalysts loaded with 2, 4, 6 and 10 wt% Pd were prepared and named as 2% Pd/Clay, 4% Pd/Clay, 6% Pd/Clay and 10% Pd/Clay respectively. To understand the phase formation, these catalysts were characterized by X-ray diffraction (XRD) technique. The obtained XRD patterns of all synthesized catalyst and also the pristine clay is shown in **Fig. 1.**

The resultant XRD pattern (**Fig. 1a**) revealed the crystalline nature of the clay with characteristic peaks of montmorillonite and quartz content **(Fig. S1)** of the supporting information.[29] The broad diffraction peaks centered at 2θ values of 40°, 46.81°, 68° and 82° correspond to the (111), (200), (220), (311) crystal planes of face centered cubic (fcc) structure of metallic Pd in accordance with JCPDS No 05-0681.[32] It is observed that as the Pd loading in clay increases, the intensity of (111) plane increase gradually (**Fig. 1 b, c, d** and **e**). This indicates the preferential growth of (111) plane.[33] From the XRD pattern as shown in **Fig. 1**, neither peak shifting of d(001) plane of clay nor its disappearance was

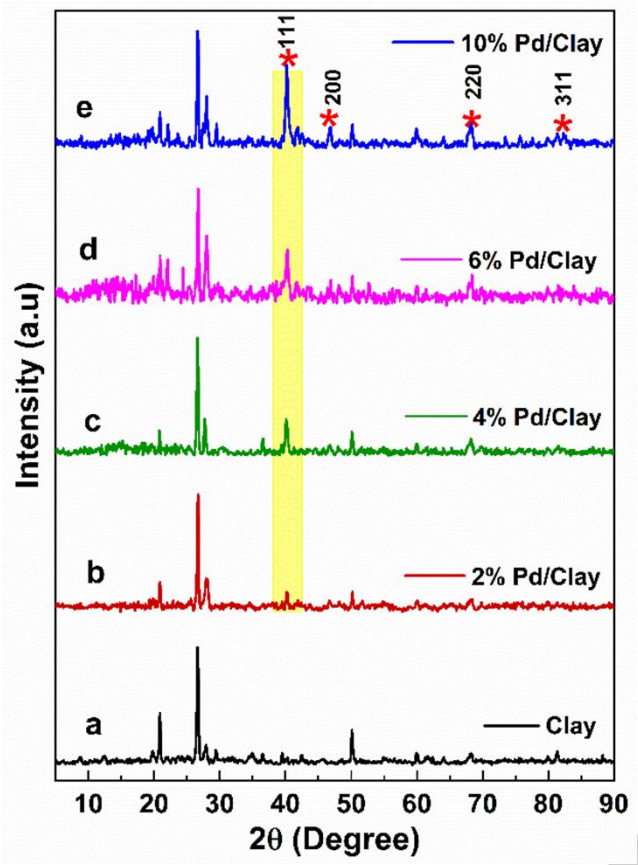

Figure 1. XRD patterns of Clay and Pd/Clay catalysts catalyst loaded with different wt %Pd.

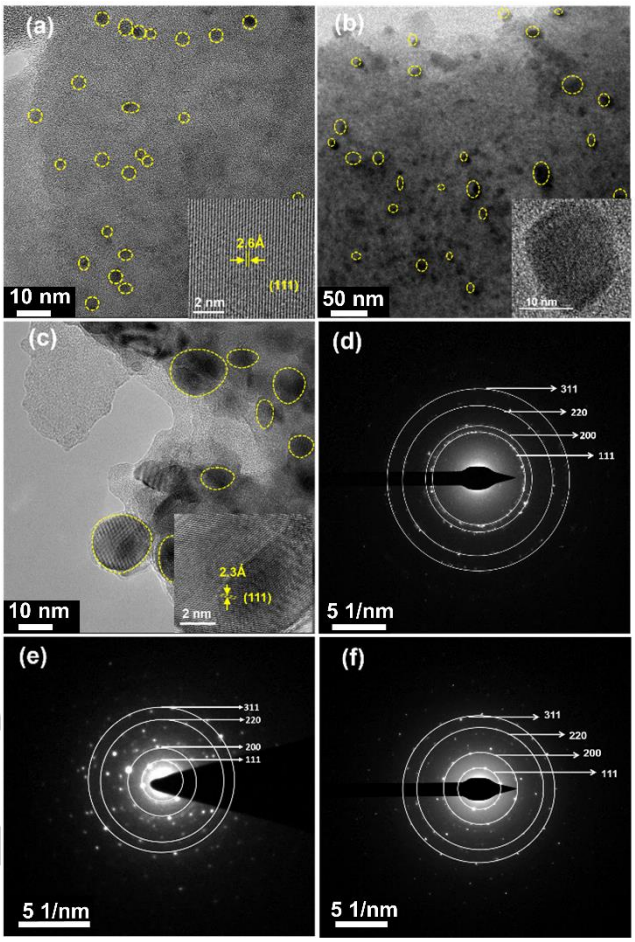

Figure 2. TEM images of Pd loaded clay with 2 wt%, 6 wt% and 10wt% (a-c) and their SAED pattern respectively (d-f).

observed as earlier reported in literatures.[33-34] This may be due to spacing irregularity of clay layers upon intercalation resulting in presence of Pd particles on the clay layers. Additionally, the intensity of (001), (002) and (003) planes of the montmorillonite clay is decreased significantly upon metal intercalation (see **Fig. S1 b**, **c** and **d**), which indicated the effective metal intercalation occurs during wet impregnation aided by dilute nitric acid.

Further, the intercalation, surface morphology and elemental distribution of Pd over the clay surface were confirmed by transmission electron microscopy (TEM) as shown in **Fig. 2.** From the **Fig. 2 a, b** and **c** (for 2% Pd/Clay, 6% Pd/Clay and 10% Pd/Clay), spherical NPs of Pd with size around 2−20 nm were found and the NPs are well-dispersed on the clay support. The interplanar d-spacing of 2.6Å and 2.3Å which corresponds to the Pd(111) plane for 2% Pd/Clay and 10% Pd/Clay respectively. [35] Additionally, the detailed morphological studies and intercalation properties of clay and Pd incorporated clay (for 2% Pd/Clay, 6% Pd/Clay and 10% Pd/Clay) can be understood from TEM image (**Fig. 3).** The layered structure of pristine clay of distinct layers can be evidently seen and marked in **Fig. 3(a).** Furthermore, **Fig. 3 (b), (c), (d)** demonstrates that Pd intercalation has not significantly affected the clay-layer structure.

The tubular structure observed in Fig. 3d may be attributed to the presences of traces of halloysite content which is not evident from the XRD analysis.[20a] Moreover, Pd NPs were found to be present inside and outside of the clay layers, which confirms the successful intercalation of Pd onto the clay.[36] The Selected Area Electron Diffraction (SAED) patterns for the samples (**Fig. 2 d, e**

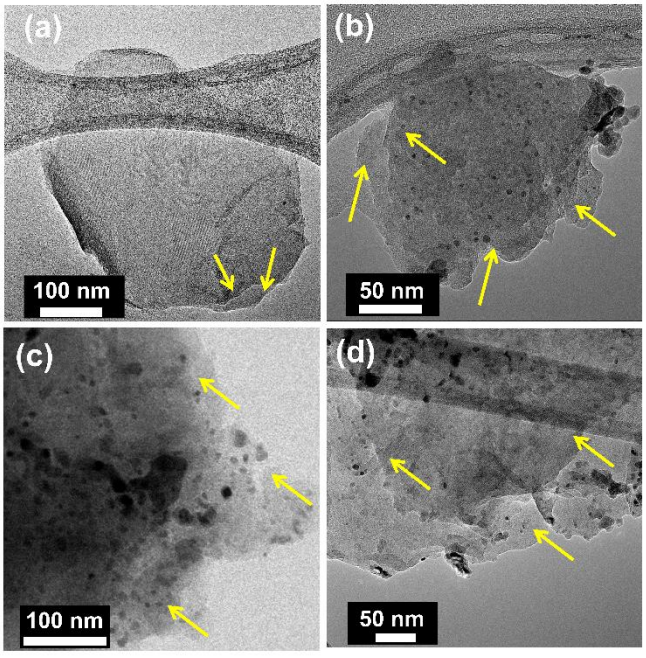

Figure 3. TEM images of clay (a) 2 wt% Pd (b) 6 wt% Pd (c) 10 wt% Pd (d) loaded clay

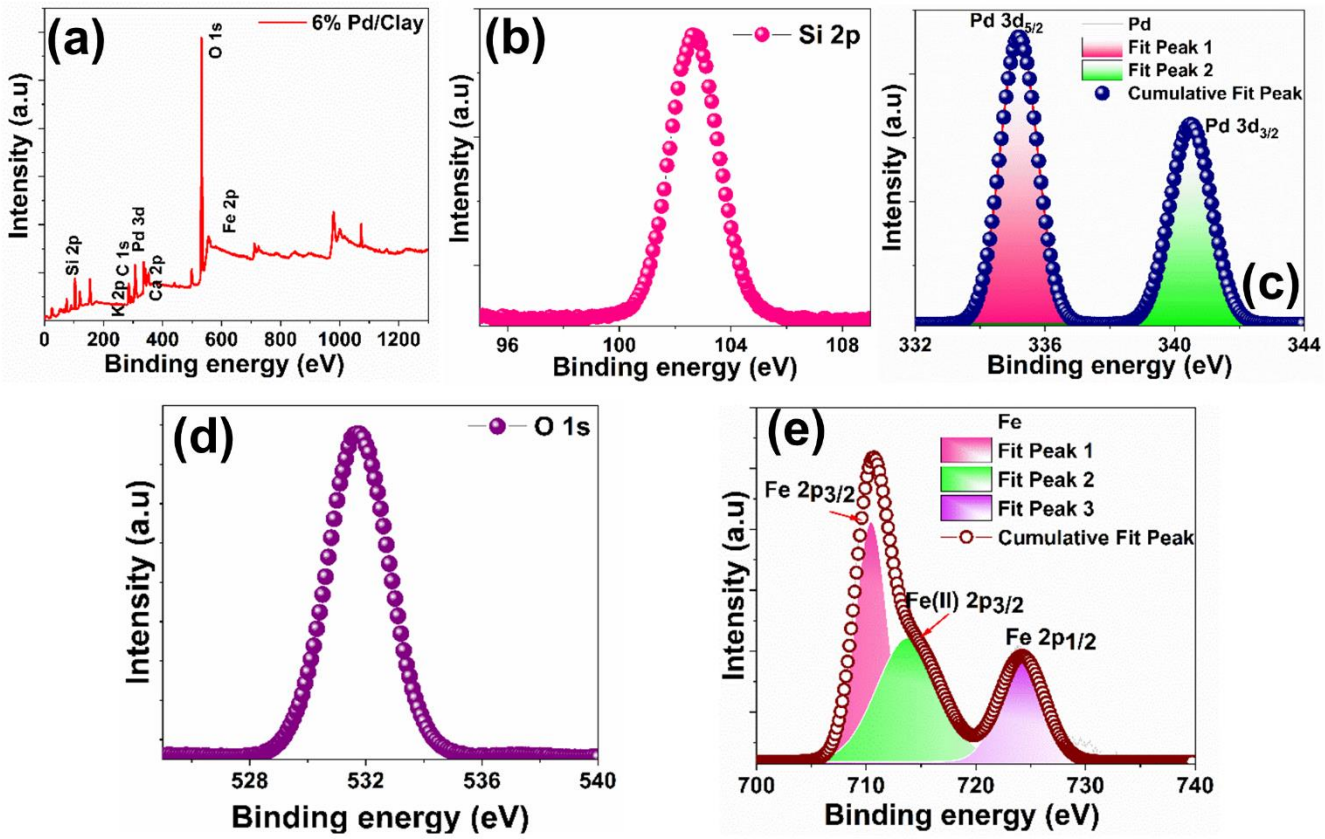

Figure 4. (a) XPS Survey scan of 6 wt% Pd/Clay catalyst, XPS core level spectra of 6 wt% Pd/Clay catalyst showing (b) Si 2p (c) Pd 3d (d) O 1s (e) Fe 2p.

and f) showed bright small spots forming rings of Pd (111), Pd (200) and Pd (220) planes which revealed the polycrystalline nature of catalyst.[37] The presence of active metal Pd and the other metals from the clay such as Fe, Si, O, Ca and K were identified from the EDS spectra of the catalyst and were given in **Fig. S2**.

The surface elemental composition and oxidation state of active metals in clay catalyst were investigated by using X-ray photoelectron spectroscopy (XPS) as shown in **Fig. 4**. XPS survey scan (**Fig. 4a**) revealed the presence of Pd, Fe, Si, Ca, K and O species in the catalyst which is corroborated with the EDS data. The C 1s peak obtained at 284.8 eV was used for spectral calibration. Core level spectra of palladium in **Fig. 4c** revealed two peaks at binding energy 335.2 and 340.48 eV which corresponds to $3d_{5/2}$ and $3d_{3/2}$ electronic states of Pd(0) respectively.[38] No other peaks for Pd^{2+} were observed for the sample. The core spectra for Fe (**Fig. 4e**) showed two peaks at 710.552 and 723.80 eV respectively which were assigned as Fe $2p_{3/2}$ and Fe $2p_{1/2}$.[39] A satellite peak of Fe(II) $2p_{3/2}$ is found at binding energy of 714.05 eV. The Si 2p spectra (**Fig. 4b**) present a single band around 102.6 eV which is characteristic of silicon bonded to carbon and/or oxygen.[40] The O 1s core spectra displayed a single strong peak around 532 eV in **Fig. 4d** which is related to the silicon oxygen bonding (Si-O-Si) present in silica and shows good agreement with clay minerals studies.[41]

To understand the reducibility of the synthesized catalyst temperature programmed reduction (H_2-TPR) analysis was carried out and the TPR profiles for clay and Pd loaded clay catalyst were shown in **Fig. 5**. For pure Montmorillonite clay sample, no reduction peak was found below 450 ℃. However, all the Pd loaded clay catalysts exhibited one strong negative peak at 65-72 °C, which is characteristic of the decomposition of the β-PdH phase formed at RT by adsorption of hydrogen on the Pd based catalyst as illustrated by equation:[42]

$PdO + H_2 \rightarrow \beta PdH \rightarrow Pd(s) + H_2$

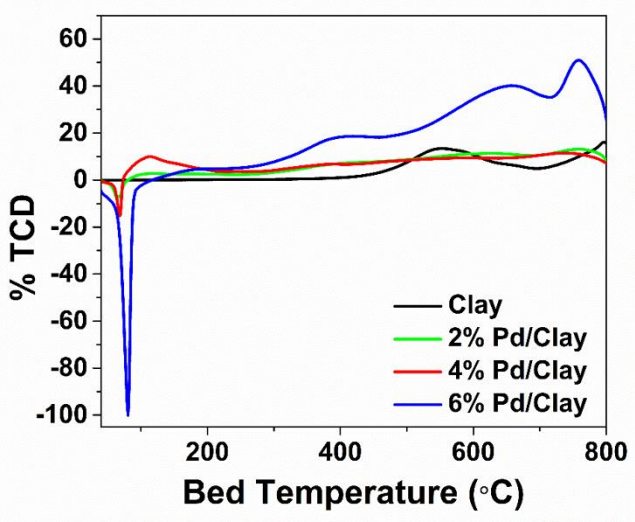

Figure 5. H_2 TPR Profile of clay and unhydrogenated Pd/Clay catalysts with different wt% Pd

Intensity and position of this negative peak depend on the size of supported Pd metal particles. It can be observed from TPR profile that as the palladium loading is increased, the fraction of palladium increases resulting in more pronounced negative peak. H_2 consumption between 100 and 200 °C is clearly observed for Pd 2% and Pd 4% resulting from the reduction of small nanosized PdO species and is supported from TEM analysis.[43] Reduction process in high temperature range of 250–550 °C range is due to the reduction of PdO particles interacting strongly with the surface of the support.

N_2 adsorption-desorption isotherms, adsorption plots and BJH pore distribution curve at 77 K of the initial montmorillonite and the metal intercalated clays are shown in **Fig. S3**, which displayed typical type IV N_2 isotherms with an H3 type hysteresis loop according to the BDDT classification, and confirm the mesoporous layered nature of the clay.[44] . Compared to the pristine clay sample, there is decrease in the N_2 adsorption capacity of palladium loaded clay and the associated surface area from 44.547m^2/g in clay to 16.519m^2/g in 6 wt% Pd/Clay. This could be ascribed to the space occupied by metallic Pd on the clay surface. Further, the appreciable increase in the average pore size of the Pd incorporated clay (from 25.25 Å (2 wt% Pd/Clay) to 165.7 Å (10 wt% Pd/Clay)) as compared to pristine clay (15.83 Å) as shown in **Table S1** indicates that the occurrence of Pd NPs in interlayered clay.[36] A huge increase of the average pore size is observed for 10 wt% Pd/Clay. This is because, with increase in metal loading, the smaller pores are closed, while larger pore size are only available for physisorption.

Table 1: Catalytic hydrogenation of 3-diphenyl prop-2-en-1-imine with prepared catalyst[a]

Entry	Catalyst	Reaction time [h]	Temperature [°C]	Pressure [bar]	Conversion [%]	Selectivity [b] A%	Selectivity[c] B%	Substrate to Metal ratio	TOF [h^{-1}]
1	2% Pd/clay	5	100	15	84 ± 0.9	84 ± 0.9	-	1: 4 x 10-3	39.23
2	2% Pd/clay	8	100	15	97 ± 0.8	97 ± 0.8	-	1: 4 x 10-3	28.26
3	2% Pd/clay	12	100	15	100	100	-	1: 4 x 10-3	19.25
4	2% Pd/clay	12	70	15	98 ± 0.6	98 ± 0.6	-	1: 4 x 10-3	18.98
5	2% Pd/clay	12	50	15	87 ± 0.5	85 ± 0.2	2 ± 0.3	1: 4 x 10-3	16.49
6	4% Pd/clay	3	100	15	84 ± 1	84 ± 1	-	1: 9 x 10-3	29.61
7	4% Pd/clay	5	100	15	100	100	-	1: 9 x 10-3	20.91
8	4% Pd/clay	8	100	15	100	100	-	1: 9 x 10-3	13.07
9	4% Pd/clay	10	100	15	100	100	-	1: 9 x 10-3	10.45
10	6% Pd/clay	5	100	15	100	100	-	1: 11 x 10-3	17.62
11	6% Pd/clay	5	100	12	100	100	-	1: 11 x 10-3	17.62
12	6% Pd/clay	5	100	10	100	100	-	1: 11 x 10-3	17.62
13	6% Pd/clay	3	100	12	100	100	-	1: 11 x 10-3	29.38
14	6% Pd/clay	3	100	7	100	100	-	1: 11 x 10-3	29.38
15	6% Pd/clay	3.5	100	5	100	100	-	1: 11 x 10-3	25.18
16	6% Pd/clay	3	100	5	96 ± 0.5	92 ± 0.7	3 ± 0.5	1: 11 x 10-3	27.24
17	6% Pd/clay	3	50	5	96 ± 0.4	90 ± 0.1	6 ± 0.2	1: 11 x 10-3	26.46
18	10% Pd/clay	5	100	15	100	100	-	1: 18 x 10-3	10.60
19	6% Pd/SiO2	5	100	5	88 ± 0.5	80 ± 0.5	7 ± 0.6	1: 1 x 10-3	14.19
20	6% Pd/Al2O3	5	100	5	89 ± 0.6	86 ± 0.5	3 ± 0.4	1: 12 x 10-3	15.20

[a] Reaction was performed with 0.5g Schiff base and 0.05g prepared catalyst with 10 ml methanol under varied temperature and pressure condition

[b] A = N-(3-phenylpropyl) aniline, [c] = N,3-diphenyl propan-1-amine

Thermogravimetric analysis (TGA) revealed the thermal stability of prepared catalyst and is shown in **Fig. S4**. TGA profile of processed clay show weight loss due the removal of the physisorbed water (below 100 °C), loss of the strongly bonded water molecules existing in the first coordination sphere of the interlayer ions (100-500 °C) and the loss of structural hydroxyl groups (500-900 °C).[45] TGA analysis of palladium intercalated catalyst revealed that catalysts with higher metal loadings (Pd 6 wt% and Pd 10 wt%), were stable up to 900 °C with slight initial weight reduction, which could be ascribed to loss of water molecules.[46] However, the significant weight loss was observed

with less metal loading particularly for Pd 2% and Pd 4%, which indicates that catalyst with higher metal loadings are more thermally stable. The maximum weight loss (%) was observed in 4 wt% Pd/Clay probably owing to the weakening of bonds in the clay in this case. The FT-IR spectrum of clay and palladium intercalated clay is recorded and is shown as in **Fig. S5** and it exhibited the presence of O−H bonds at 3627 cm^{-1} (OH stretching) and 3408 cm^{-1} (H-O-H stretching) corresponds to the hydroxy groups of clay and interlayer water molecules A peak at 1629 cm^{-1} was detected for O−H bending. The presence of silica is represented by broad and intense peak detected at 1018 cm^{-1} (Si-O-Si stretching).[47] Broadly, quartz presence is identified in the wavenumber region from 1200 – 500 cm^{-1}. The peak intensities due to O-H bonds were reduced after wet impregnation due to dihydroxylation caused by nitric acid.

Optimization of reaction parameters

The effects of reaction parameters (catalyst loading, reaction time, temperature and H_2 pressure) were studied to optimize the hydrogenation of 3-diphenyl prop-2-en-1-imine to 3-phenylpropylaniline as shown in **Table 1**. In order to identify the appropriate amount of palladium, the influence of different catalytic loading (2, 4, 6 and 10 wt%) was investigated. Increasing the metal loading leads to increase in conversion efficiency. It can be seen from **Table 1**, in case of lower metal loading of 2 wt% Pd/Clay, complete conversion was only achieved at the extended reaction of 12 h (**Table 1**, exp no. 3). In comparison, at higher metal loading (4 wt% Pd/Clay), it occurs within a shorter reaction period of 5 h (**Table 1**, exp no. 7). This is attributed to the increase in the available active sites with an increase in palladium content.[21] The influence of variation in reaction time on conversion of 3-diphenyl prop-2-en-1-imine was also studied. It was found that in case of 2 wt% Pd/Clay, conversion of 3-diphenyl prop-2-en-1-imine was raised from 84.66% to 97.84% with reaction time increased from 5 h to 8 h (**Table 1**, exp no 1, 2) at 100 °C and 15 bar pressure. Interestingly, increasing the reaction time further to 12 h results in the complete conversion (**Table 1**, exp no. 3). To understand the impact of temperature on conversion and selectivity of the reaction, the temperature was varied in range 50 -100 °C. It was observed that with a change in temperature, both the conversion and selectivity gets affected. For 2 wt% Pd/Clay, it has been seen that complete conversion occurs at 100 °C with reaction time of 12 h, but as the temperature is decreased to 70 °C, there is a decrease in conversion to 98.60% (**Table 1**, exp no. 4). When the temperature is further decreased to 50 °C the conversion value decreases to 87.94% with a decrease in selectivity towards 3-phenylpropylaniline denoted by selectivity A% (**Table 1**, exp no. 5). Another important variable that plays a crucial role in catalytic activity in liquid-phase hydrogenation reaction is H_2 pressure. As the H_2 pressure increases, the dissolved concentration of H_2 in reaction mixture rises resulting in the high conversion values.[48] Thus, maintenance of optimum pressure is a key to obtain high yield product. For 6 wt% Pd/Clay catalyst, complete conversion is achieved despite the pressure is decreased from 15 bar to 10 bar (**Table 1**, exp no. 10-12). To further investigate the optimized reaction conditions, H_2 pressure and reaction time were decreased simultaneously and their effect on the conversion and selectivity was examined at 100 °C. To our delight, for 6 wt% Pd/Clay, complete hydrogenation of 3-diphenyl prop-2-en-1-imine occurs with 3-phenylpropylaniline as the sole product, when the H_2 pressure was as low as 5 bar with reaction time 3.5 h (**Table 1**, exp no.15). When the time is further reduced to 3 h, nearly complete conversion was obtained but with the presence of side product represented by Selectivity B% (**Table 1**, exp no. 16). Moreover, the control experiment for the SiO_2 and Al_2O_3 loaded with 6% Pd/Clay was performed and the complete conversion was not obtained as shown in **Table 1**, entry 19 and 20 respectively. This clearly indicates the advantage of clay as a support in comparison to SiO_2 and Al_2O_3. From **Table 1**, it is understood that the proposed catalyst is cost effective and exhibits excellent reactivity towards imine hydrogenation. Here, the intrinsic properties of the clay support have played a significant role in improving the catalytic performance. During the hydrogenation process, firstly the molecular H_2 binds with the Pd surface resulting in its dissociation to form H atoms that occupy the octahedral holes within the Pd surface. These adsorbed H atoms interact with the substrate imine, where Pd intercalated clay provides the working surface for hydrogenation reaction. This is according to the hydrogenation studies based on Horiuti–Polanyi mechanism,[49] which suggest C=C bonds adsorption on the catalyst form two M-C chemical bonds, which leads to a classical three-centered transition state (C, M, H). Further identification of the reaction products, calculation of conversion and selectivity were done by comparing GC chromatograms and NMR data of imines and product (**Fig. S6, S7**). A comparison between conversion and yields of as prepared Pd/Clay catalyst and previously reported transition metal catalyst is given (**Table S2**).

From **Scheme 1**, it can be observed that the expansion of interlayer spacing in clay allows the formation of Pd NPs with highly faceted Pd (111) plane which is supported by XRD analysis (**Fig. 1**). The result obtained is corroborated to Zheng and coworkers.[50] According to their report, the hydrogenation reaction by Pd nanocrystals is facet-dependent catalysis reaction. To further substantiate the reactivity of catalyst, a study of imine-mixed catalyst was performed. In this regard, an equal amount of 2-diphenyl prop-2-en-1-imine and highly reactive 6 wt% Pd/Clay catalyst were mixed in the presence of methanol at 10 bar H_2 pressure for 2 h at RT and then methanol was air-dried at 80 °C overnight. The XRD patterns of imine-mixed clay catalyst (**Fig. 6a**) shows weakly intense characteristic Pd (111) peak compared to the pristine catalyst, indicating the strong imine adsorption on the Pd surface at RT.

This signifies the considerable role of Pd (111) plane in determining catalytic activity.[51] This strong metal-substrate interaction enables the activation of C=N and C=C bonds for effective hydrogenation. The IR spectrum of imine-mixed 6 wt% Pd/Clay (**Fig. 6b**) shows the narrowing of IR bands to give sharper peaks which again confirm the strong adsorption of imines on Pd surface.

Reusability and metal leaching studies

After demonstrating the reactivity of catalyst, reusability was ascertained to determine the stability of the catalyst.[52] To do the reusability test, the catalyst was recovered after the hydrogenation reaction. The obtained catalyst were washed with methanol three times to extract the whole reaction products. The remaining catalyst obtained was dried at 60 °C and tested for further hydrogenation reaction under optimized conditions up to 5 cycles. The comparative XRD patterns of 6 wt% Pd/Clay catalyst are shown in (**Fig. S8**) for fresh catalyst and reused catalyst after 3 and 5 cycles. There was no significant difference in the XRD patterns of fresh and reuse catalysts.

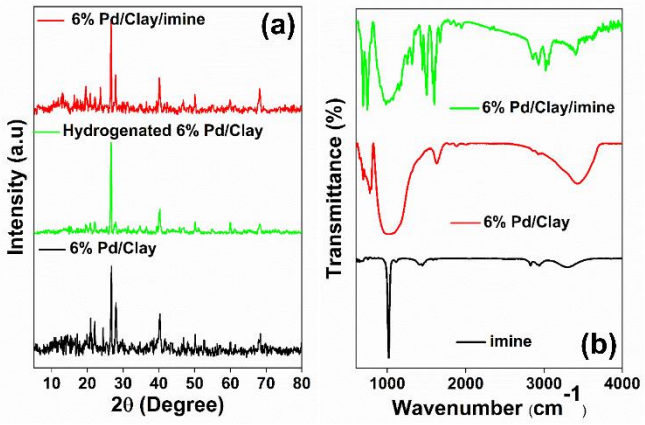

Figure 6. (a) XRD spectra of 6 wt% Pd/Clay, imine-mixed 6 wt% Pd/Clay and its hydrogenated product. (b) FTIR spectra of prepared imine, 6 wt% Pd/Clay and 6 wt% Pd/Clay/imine.

Metal leaching experiments were also conducted for 6%Pd/Clay catalyst. For these, the hydrotreatment reaction was carried out with 5g substrate and 500 mg catalyst using 100 mL methanol (at 100 °C, 5 bar H_2 pressure at 3.5 h). Upon completion of the reaction, the liquid product was separated from catalyst through centrifugation. These are analysed by ICP-OES measurement for the palladium leaching content. The remaining catalyst was washed with methanol, dried and was used in subsequent five cycles. During each cycle, the amount of the catalyst and the amount of palladium in the product were analysed and which is given in **Table S3** in the Supporting Information. The amount of Pd leaching in the separated product after each cycle was found to be less than 0.5 ppm. Consequently, a small drop in the conversion values was obtained after the second cycle. After the third cycle, the conversion value is decreased to 94%. which is probably due to the catalyst lost during the centrifugation process and metal leaching after the hydrogenation reaction. The actual metal loading and leaching of metal is examined by ICP-OES analysis and the obtained results is shown in **Table S3**,**Table S4** and **Table S5**. These experiment results indicates the excellent stability as well as efficiency of the Pd/Clay catalysts for the hydrogenation of imine under mild reaction conditions.

Conclusion

In conclusion, a green and sustainable natural clay-based catalytic system is developed via easy one-step wet impregnation method and applied for hydrogenation of imines. Here, the clay plays a vital role as the support for the immobilisation of Pd NPs owing to its intrinsic properties. The interlayered structure of the clay and effective intercalation was confirmed by various characterization techniques such as XRD, TEM and BET analysis. Among the different Pd loaded clay catalysts, 6 wt% Pd loading showed the good stability and exhibits excellent high catalytic performance for the hydrogenation of imines. This is attributed to the dominating highly faceted Pd (111) plane in the interlayered clay structure. Hydrotreatment studies revealed that reaction parameters play a crucial role in determining activity and selectivity. The obtained GC results established that under optimized conditions of 5 bar H_2 pressure for 3.5 h, 6 wt% Pd/Clay exhibited 100% conversion of the imine with 100% selectivity of 3-phenylpropylaniline without any side products. The catalyst is stable and can be reused over five cycles. Owing to its cost effectiveness, simple synthesis procedure and high catalytic activity, this study would help in crafting rational approaches to explore other hydrogenation reactions by bridging the two disciplines of metal NPs and clay systems.

Experimental Section

Materials

Natural montmorillonite clay was obtained from a native source in Rajasthan, India. Palladium nitrate hydrate (99.9 %) was procured from Alfa Aesar. Extra dry methanol, Aniline and Nitric acid were purchased from Acros organics Fisher Scientific. Trans Cinnamaldehyde was obtained from Spectrochem. Ethanol was obtained from Changshu Hongsheng Fine Chemical Co.Ltd.

Preparation of schiff base

Schiff base, 3-diphenyl prop-2-en-1-imine is synthesized by condensation of Equimolar concentration of Trans Cinnamaldehyde and Aniline (0.01 mol) in ethanol (5ml), and the resultant mixture was gently stirred at ambient temperature. The progress of the reaction was monitored by TLC. The resultant mixture was left undisturbed at RT for half an hour until small yellowish crystals start growing. It was then carefully set in an ice bath to complete the crystallization process. The chilled solution was then filtered through vacuum filtration to isolate the pure crystals, and the crystals were washed with cold ethanol solvent.

Preparation of catalysts

A series of palladium loaded (2, 4, 6, 10 wt%) on to clay catalysts were prepared following the procedure reported earlier.[19] Briefly, the clay was sequentially treated with 1N HNO_3 and 1N NH_4OH for 12 h each at RT. The resulting clay was washed thoroughly with deionized water and dried overnight in an oven at 120 ℃ to be utilized as the solid support. Palladium metal was incorporated by using the wet impregnation method. The required amount of Palladium(II) nitrate hydrate in 3N HNO_3 (10 mL) was impregnated onto clay support (1g), and the mixture was dried at 120℃ with incessant stirring until it forms a thick paste. The powdered material was calcined at 500 ℃ for 5 h (flow rate: 2 mL/min) under a nitrogen atmosphere, succeeded by reduction of the metal at 300 ℃ for 3 h (flow rate: 2 mL/min) under a hydrogen atmosphere. The resulting solid was finely grinded to form a fine powder.

Characterization

X-ray diffraction (XRD) measurements were performed using D8 Advance diffractometer (Bruker, U.S.A.), with Cu Kα (λ = 1.54Å) as the radiation source at 40 kV voltage and 40 mA tube current for scanning diffraction angle in the range of 5 to 90°. For morphological and elemental composition studies, High-resolution Transmission Electron Microscope (HR-TEM) analysis was carried out using TALOS F200S G2 instrument. The hydrogen temperature-programmed reduction (H_2-TPR) was performed on a Chemisorption Analyzer (AMI-300, Altamira Instruments) equipped with a thermal conductivity detector (TCD). For H_2 TPR studies, pre-treatment at rate 10 °C per min under helium for 1 hr is done until it reaches 150 °C, then it is cooled to ambient temperature. A mixture of H_2 (5%) + He (95%) was flowed at a rate of 30 mL/min to be used as reducing agent and heated to 800 °C at 10 °C/min and maintained for 30 min and TPR profile was monitored in a range of 30-800 °C. Autosorb-1Q-MP-XR (Quantachrome Instruments, USA) was used for adsorption-desorption measurement to perform surface area and porosity analysis. N_2 gas was

taken as carrier gas with 99.995% purity. The sample was degassed under a vacuum at 180 °C for 3 h, which is followed by nitrogen adsorption−desorption analysis at -196 °C. Thermogravimetric (TGA) analysis was done on Simultaneous Thermal Analyzer (STA) – 6000 from Perkin Elmer under nitrogen atmosphere at a flow rate of 19.8 mL/min and pressure 3 bar with a heating rate of 10 °C min^{-1}. Fourier transformed infrared spectroscopy (FTIR) from Bruker (Vertex, 70V+PMA50) was used for recording the FTIR spectrum from 400 cm^{-1} to 4000 cm^{-1} at room temperature (RT) with 32 scan performance. The surface composition and the elemental states were determined with X-ray photoelectron spectroscope (XPS) by an Omicron NanoTechnology GmbH (Oxford Instruments) equipped with the monochromatic Al Kα radiation. The charge correction was done with reference to standard carbon 1s peak attained at 284.1 eV. Nuclear Magnetic Resonance (NMR) spectra were recorded on an 11.2 Tesla Bruker operating at 500 MHz in $CDCl_3$. Gas chromatography (GC) analysis was performed by using PerkinElmer Clarus 580 gas chromatograph equipped with Elite-5 capillary column with 30 m length, 0.10 µm film thickness, 0.25 mm inner diameter and a temperature limit of −60 to 325/350 °C.

Hydrogenation of imine

All the hydroprocessing was carried out in a high pressure vessel equipped with a steel container of capacity 250mL provided by Amar Equipments Pvt. Ltd. The catalyst (50 mg), as prepared 3-diphenyl prop-2-en-1-imine (500 mg) and dry methanol (10ml) were taken in the air-dried container. A vacuum was created in the container, accompanied by purging the hydrogen gas. The reaction temperature was raised from 25 ℃ at 5 ℃ min^{-1} to attain the required temperature (50 - 100 ℃) prolonged for several hours for time- dependent studies at varied pressure. At the end of the catalytic test, the reactor was allowed to attain RT and depressurized. The mixture was centrifuged and the liquid fraction was separated. Further, methanol (10 mL × 2) was added to the catalyst, stirred, centrifuged to extract most of the product. Conversion and selectivity of reaction were measured by GC equipped with FID detector. The product formation was further supported by ^{1}H NMR, ^{13}C NMR spectroscopy and mass spectroscopy.

Recycling tests

To do the reusability test, the used catalyst for hydrogenation reaction was recovered after the reaction by centrifugation. The obtained catalyst were washed with methanol three times to extract the whole reaction products and unreacted substrate if any. The obtained catalyst was dried overnight at 60 °C in vacuum oven. These were and tested further for hydrogenation reaction as explained above under the optimized reaction conditions up to 5 cycles.

Leaching Tests

The leaching tests were carried out in a Berghof HR-1000 high pressure reactor equipped with a teflon container of 1000 mL capacity. The liquid product obtained after the hydrogenation reaction of 5 g 3-diphenyl prop-2-en-1-imine with 0.5g of 6% Pd/Clay catalyst at 100 °C, 5 b pressures for 3.5 hr was analyzed by ICP-OES.

Acknowledgements

The authors express their gratitude toward DBT-PAN IIT Centre for Bioenergy (BT/EB/PANIIT/2012) for financial assistance. We also thank Centre for Advanced Scientific Equipment (CASE)-IIT Jodhpur, Scientium Analyze Solutions for XPS, CeNS Bangalore for TEM analysis. We also thank Mr. Bhagirath for helping in calculations and proof reading.

Keywords: • heterogeneous catalysis • hydrogenation • imines • montmorillonite clays • Pd nanoparticles

References

[1] a) M. Poyatos, F. Márquez, E. Peris, C. Claver, E. Fernandez, *New J. Chem.* **2003**, *27*, 425-431; b) C.-J. Li, B. M. Trost, *Proc. Natl. Acad. Sci. U. S. A.* **2008**, *105*, 13197; c) O. V. Kharissova, B. I. Kharisov, C. M. O. González, Y. P. Méndez, I. López, *R. Soc. Open Sci.* **2019**, *6*, 191378; d) J. H. Clark, *Green Chem.* **1999**, *1*, 1-8.

[2] P. J. Deuss, K. Barta, J. G. de Vries, *Catal. Sci. Technol.* **2014**, *4*, 1174-1196.

[3] a) R. Nie, M. Chen, Y. Pei, B. Zhang, L. Qi, J. Chen, T. W. Goh, Z. Qi, Z. Zhang, W. Huang, *ACS Sustainable Chem. Eng.* **2018**, *7*, 3356-3363; b) S. S. Joshi, A. Bhatnagar, V. V. Ranade, in *Ind. Catal. Processes Fine Spec. Chem.* (Eds.: S. S. Joshi, V. V. Ranade), Elsevier, Amsterdam, **2016**, 317-392.

[4] a) J. M. Fraile, N. García, C. I. Herrerías, M. Martín, J. A. Mayoral, ACS Catal. **2011**, *2*, 56-64; b) D. Macquarrie, in *Heterogenized Homogeneous Catalysts for Fine Chemicals Production: Materials and Processes* (Eds.: P. Barbaro, F. Liguori), Springer Netherlands, Dordrecht, **2010**, 1-35; c) M. J. Climent, A. Corma, S. Iborra, Chem. Rev. **2011**, *111*, 1072-1133.

[5] a) H. Bauer, M. Alonso, C. Färber, H. Elsen, J. Pahl, A. Causero, G. Ballmann, F. De Proft, S. Harder, *Nat. Catal.* **2018**, *1*, 40-47; b) X. Jv, S. Sun, Q. Zhang, M. Du, L. Wang, B. Wang, *ACS Sustainable Chem. Eng.* **2019**, *8*, 1618-1626.

[6] a) Y. Obora, T. Ohta, C. L. Stern, T. J. Marks, *J. Am. Chem. Soc.* **1997**, *119*, 3745-3755; b) H. Elsen, J. Langer, M. Wiesinger, S. Harder, *Organometallics* **2020**.

[7] Q. A. Chen, Z. S. Ye, Y. Duan, Y. G. Zhou, *Chem Soc Rev* **2013**, *42*, 497-511.

[8] P. Das, P. P. Sarmah, B. J. Borah, L. Saikia, D. K. Dutta, *New J. Chem.* **2016**, *40*, 2850-2855.

[9] Y.-F. He, J.-T. Feng, Y.-Y. Du, D.-Q. Li, ACS Catal. **2012**, *2*, 1703-1710.

[10] P. P. Sarmah, D. K. Dutta, *Green Chem.* **2012**, *14*.

[11] C. Wang, L. Wang, J. Zhang, H. Wang, J. P. Lewis, F.-S. Xiao, *J. Am. Chem. Soc.* **2016**, *138*, 7880-7883.

[12] F. Yang, C. Chi, S. Dong, C. Wang, X. Jia, L. Ren, Y. Zhang, L. Zhang, Y. Li, *Catal. Today* **2015**, *256*, 186-192.

[13] E. J. García-Suárez, P. Lara, A. B. García, M. Ojeda, R. Luque, K. Philippot, *Appl. Catal., A* **2013**, *468*, 59-67.

[14] S.-Y. Chen, L. Attanatho, T. Mochizuki, Q. Zheng, M. Toba, Y. Yoshimura, P. Somwongsa, S. Lao-Ubol, *Adv. Porous Mater.* **2016**, *4*, 230-237.

[15] T. J. Pinnavaia, *Science* **1983**, *220*, 365-371.

[16] a) D. Dutta, D. K. Dutta, Appl. Catal., A **2014**, *487*, 158-164; b) T. Hayakawa, M. Minase, K.-i. Fujita, M. Ogawa, , Ind. Eng. Chem. Res. **2016**, *55*, 6325-6330.

[17] D. Manikandan, D. Divakar, T. Sivakumar, *Catal. Commun.* **2007**, *8*, 1781-1786.

[18] a) B. S. Kumar, A. Dhakshinamoorthy, K. Pitchumani, *Catal. Sci. Technol.* **2014**, *4*, 2378-2396; b) G. Qiu, C. Huang, X. Sun, B. Chen, *Green Chem.* **2019**, *21*, 3930-3939.

[19] F. M. T. Luna, J. A. Cecilia, R. M. A. Saboya, D. Barrera, K. Sapag, E. Rodriguez-Castellon, C. L. Cavalcante, Jr., *Materials (Basel)* **2018**, *11*.

[20] a) Y. Zheng, L. Wang, F. Zhong, G. Cai, Y. Xiao, L. Jiang, *Ind. Eng. Chem. Res.* **2020**, *59*, 5636-5647; b) C. B. Molina, A. H. Pizarro, J. A. Casas, J. J. Rodriguez, *Appl. Catal., B* **2014**, *148-149*, 330-338; c) S. Barama, C. Dupeyrat-Batiot, M. Capron, E. Bordes-Richard, O. Bakhti-Mohammedi, *Catal. Today* **2009**, *141*, 385-392; d) L. C. A. Oliveira, R. M. Lago, J. D. Fabris, K. Sapag, *Appl. Clay Sci.* **2008**, *39*, 218-222; e) G. Ngnie, G. K. Dedzo, C. Detellier, *Dalton Trans.* **2016**, *45*, 9065-9072.

[21] A. B. Gawade, M. S. Tiwari, G. D. Yadav, *ACS Sustainable Chem. Eng.* **2016**, *4*, 4113-4123.

[22] S. Sreekumar, S. Xavier, A. Govindan, R. E. Thampikannu, K. Vellayan, B. González, *Res. Chem. Intermed.* **2020**, *46*, 4529-4542.

[23] N. S. Date, R. C. Chikate, H.-S. Roh, C. V. Rode, *Catal. Today* **2018**, *309*, 195-201.

[24] Y. H. Ahmad, A. T. Mohamed, K. A. Mahmoud, A. S. Aljaber, S. Y. Al-Qaradawi, *RSC Adv.* **2019**, *9*, 32928-32935.

[25] P. R. Boruah, P. S. Gehlot, A. Kumar, D. Sarma, *Mol. Catal.* **2018**, *461*, 54-59.
[26] K. Vellayan, B. González, R. Trujillano, M. A. Vicente, A. Gil, *Appl. Clay Sci.* **2018**, *160*, 126-131.
[27] R. K. Loganathan, S. N. Ramachandra, Shekharappa, V. V. Sureshbabu, *ChemistrySelect* **2017**, *2*, 8059-8062.
[28] A. V. Martínez, A. Leal-Duaso, J. I. García, J. A. Mayoral, *RSC Adv.* **2015**, *5*, 59983-59990.
[29] V. K. Soni, R. K. Sharma, *ChemCatChem* **2016**, *8*, 1763-1768.
[30] V. K. Soni, P. R. Sharma, G. Choudhary, S. Pandey, R. K. Sharma, , *ACS Sustainable Chem. Eng.* **2017**, *5*, 5351-5359.
[31] M. Zeng, Y. Wang, Q. Liu, X. Yuan, S. Zuo, R. Feng, J. Yang, B. Wang, C. Qi, Y. Lin, *ACS Appl. Mater. Interfaces* **2016**, *8*, 33157-33164.
[32] G. B. B. Varadwaj, S. Rana, K. Parida, *The Journal of Physical Chemistry C* **2014**, *118*, 1640-1651.
[33] I. B. Adilina, N. Rinaldi, S. P. Simanungkalit, F. Aulia, F. Oemry, G. B. G. Stenning, I. P. Silverwood, S. F. Parker, *The Journal of Physical Chemistry C* **2019**, *123*, 21429-21439.
[34] a) Q.-Q. Hao, G.-W. Wang, Z.-T. Liu, J. Lu, Z.-W. Liu, Ind. Eng. Chem. Res. **2010**, *49*, 9004-9011; b) D. Varade, K. Haraguchi, *Langmuir* **2013**, *29*, 1977-1984.
[35] a) Z. Wu, Q. Zhu, C. Shen, T. Tan, *ACS Omega* **2016**, *1*, 498-506; b) V. Srivastava, Open Chem. **2018**, *16*, 605-613.
[36] D. Varade, K. Haraguchi, *Phys. Chem. Chem. Phys.* **2014**, *16*, 25770-25774.
[37] W. Xu, H. Sun, B. Yu, G. Zhang, W. Zhang, Z. Gao, *ACS Appl. Mater. Interfaces* **2014**, *6*, 20261-20268.
[38] a) L. Duan, R. Fu, B. Zhang, W. Shi, S. Chen, Y. Wan, *ACS Catal.* **2016**, *6*, 1062-1074; b) Y. Huang, S. Gao, T. Liu, J. Lü, X. Lin, H. Li, R. Cao, *ChemPlusChem* **2012**, *77*, 106-112.
[39] T. Yamashita, P. Hayes, *Appl. Surf. Sci.* **2008**, *254*, 2441-2449.
[40] I. Santana, A. Pepe, W. Schreiner, S. Pellice, S. Ceré, *Electrochim. Acta* **2016**, *203*, 396-403.
[41] B. J. W. J. Theo Kloprogge, *Clay Sci.* **2018**, *22*, 85-94.
[42] a) A. Aznárez, A. Gil, S. A. Korili, *RSC Adv.* **2015**, *5*, 82296-82309; b) B. Tyagi, C. D. Chudasama, R. V. Jasra, *Spectrochim. Acta, Part A* **2006**, *64*, 273-278.
[43] J. Oh, H. B. Bathula, J. H. Park, Y.-W. Suh, *Commun. Chem.* **2019**, *2*.
[44] a) M. Thommes, K. Kaneko, A. V. Neimark, J. P. Olivier, F. Rodriguez-Reinoso, J. Rouquerol, K. S. W. Sing, *Pure Appl. Chem.* **2015**, *87*, 1051-1069; b) S. Brunauer, L. S. Deming, W. E. Deming, E. Teller, *J. Am. Chem. Soc.* **1940**, *62*, 1723-1732.
[45] a) V. S. Kshirsagar, A. C. Garade, R. B. Mane, K. R. Patil, A. Yamaguchi, M. Shirai, C. V. Rode, *Appl. Catal., A* **2009**, *370*, 16-23; b) K. Motokura, S. Matsunaga, H. Noda, A. Miyaji, T. Baba, *ACS Catal.* **2012**, *2*, 1942-1946.
[46] D. Aldhayan, A. Aouissi, *Bull. Chem. React. Eng. Catal.* **2017**, *12*.
[47] S. Bentahar, M. A. Taleb, A. Sabour, A. Dbik, M. El Khomri, N. El Messaoudi, A. Lacherai, R. Mamouni, *Russ. J. Org. Chem.* **2019**, *55*, 1423-1431.
[48] W. Gong, C. Chen, Y. Zhang, H. Zhou, H. Wang, H. Zhang, Y. Zhang, G. Wang, H. Zhao, *ACS Sustainable Chem. Eng.* **2017**, *5*, 2172-2180.
[49] B. Mattson, W. Foster, J. Greimann, T. Hoette, N. Le, A. Mirich, S. Wankum, A. Cabri, C. Reichenbacher, E. Schwanke, *J. Chem. Educ.* **2013**, *90*, 613-619.
[50] X. Zhao, Y. Zhao, G. Fu, N. Zheng, *Chem. Commun. (Cambridge, U. K.)* **2015**, *51*, 12016-12019.
[51] R. Kumar, B. S. Rana, R. Tiwari, D. Verma, R. Kumar, R. K. Joshi, M. O. Garg, A. K. Sinha, *Green Chem.* **2010**, *12*, 2232-2239.
[52] M. Jeganathan, A. Dhakshinamoorthy, K. Pitchumani, , *ACS Sustainable Chem. Eng.* **2014**, *2*, 781-787.

Entry for the Table of Contents

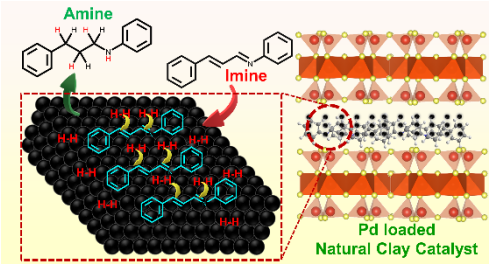

A facile and straightforward synthesis protocol using natural clay as support was demonstrated for the preparation of cost-effective Pd/Clay catalyst. Among the different loaded metal catalyst, 6 wt% Pd/Clay catalyst system displayed the maximum catalytic performance for the hydrogenation of 3-diphenyl prop-2-en-1-imine with complete conversion and 100 % selectivity to yield 3-phenyl propyl aniline under mild reaction conditions of 5 bar pressure under shorter duration of 3.5 h at 100 °C.